

Interpretation of low-energy Auger spectra from AlAs and GaAs(001): Applications to surface preparation

Stefan P. Svensson,* P. O. Nilsson, and T. G. Andersson

Department of Physics, Chalmers University of Technology, S-412 96 Göteborg, Sweden

(Received 30 August 1984; revised manuscript received 14 December 1984)

The relative positions of the low-energy Auger transitions for the III-V elements Ga, Al, In, As, P, and Sb have been estimated to enable selection of III-V compounds suitable for studies of *CVV* transitions. The surface-sensitive Auger spectra of GaAs and AlAs have been investigated in detail with emphasis on the *CVV*-type transitions. It is shown that a single-particle theory, using a bulk band structure, is sufficient to analyze the topmost (most intense) part of *CVV* transitions from the investigated group-III and -V elements. The As $M_{45}VV$ peak line shape has been studied for different surface phases. Experimentally, it was found that the line shape of the peak is sensitive to the chemical surrounding of the As atom. Hence by studying an As-rich GaAs(001) surface (grown by molecular-beam epitaxy) during desorption, the As $M_{45}VV$ line shape was found to change from mainly As to GaAs character as the polar surface changed phase. The As $M_{45}VV$ line shape was found to be different for GaAs and AlAs, a fact that has been used to detect AlAs formation during Al adsorption on GaAs. Furthermore, the accuracy of the observable part of the As $M_{45}VV$ peak as a measure of the As concentration is discussed. Upon comparison of the Ga $M_{23}M_{45}M_{45}$ peaks from metallic Ga and GaAs, it was seen that the intensity ratio between the $M_2M_{45}M_{45}$ and $M_3M_{45}M_{45}$ lines deviates from the expected value based on the statistical occupation of the M_2 and M_3 levels.

I. INTRODUCTION

Auger-electron spectroscopy (AES) is one of the most commonly used surface analytical tools today. The surface sensitivity can be enhanced by observing the low-kinetic-energy spectra. In this energy range some of the most intense transitions from, e.g., semiconductors are of the *CVV* type. Although frequently used, these transitions from III-V compounds have not before been subject to theoretical analysis. In earlier surface studies of GaAs grown by molecular-beam epitaxy (MBE), it has been shown that surface properties, such as the band bending¹ and the Schottky-barrier height after metallization,² depend on the composition of the semiconductor surface. These properties may vary also for identical surface geometries depending on the way the sample is produced.² It is thus important to realize that a MBE-produced GaAs(001) surface does not necessarily show properties that are intrinsic to an ideal (001) surface but rather that are specific to the production method used. Relating such properties to the production method and the surface composition and geometry is therefore one of the most important fields in studies of MBE surfaces. Consequently, it is highly desirable to obtain an increased understanding about what kind of surface information can be extracted from the common types of MBE instrumentation available, namely AES and reflection high-energy electron diffraction (RHEED). These facts have motivated the present analysis of the surface-sensitive low-energy spectra of III-V-compound semiconductors where we have paid special attention to the line shape of *CVV* transitions.

The paper is organized in the following way: After reporting the experimental details we investigate the low-

energy peak distribution of Auger transitions for the commonly used III-V elements. We will, in particular, consider GaAs and AlAs, discussing in detail the line shapes of the Ga $M_{23}M_{45}M_{45}$, As $M_{45}VV$, and Al $L_{23}VV$ peaks. A line shape calculation for the *CVV* peaks is presented and compared with experimentally obtained data from MBE-grown material. Finally, we discuss the general bearing of our findings on studies of MBE-grown surfaces.

II. EXPERIMENTAL DETAILS

The GaAs(001) surfaces were prepared by MBE growth in a Varian 360 system. No particular precautions were taken to minimize any adatom population of As on the surfaces. After cooling the sample to room temperature, a $c(4 \times 4)$ reconstruction was observed using RHEED. The samples were then heated stepwise in order to desorb surface As, maintaining ordered surface structures. The maximum temperature was 600 °C, at which a $c(8 \times 2)$ reconstruction was observed. No evidence for Ga precipitates was found. At each temperature, Auger spectra were recorded with a Varian single-pass cylindrical mirror analyzer (CMA) with an energy resolution of 0.3%. Spectra were digitally recorded³ in the first-derivative mode using modulation voltages of 0.5 or 1 V. A similar procedure was used for growth of AlAs. This material was heavily doped with Si to avoid charging effects. For line-shape comparison a pure-As Auger spectrum was obtained from a cooled (~ 0 °C) Mo-substrate holder which had been exposed for ~ 10 min to an As₄ flux. A Ga spectrum was obtained by evaporation of a thick Ga layer on an oxidized Si crystal. Si was chosen here to avoid any

possible incorporation of As in the film.

As will be seen in the further analysis of the spectra, peaks appear in many III-V compounds such as GaAs and AlAs, over the entire energy range of interest. Because no free parts of the background are available that could be used for fitting of a functional background model, background and peak fitting must be treated in the same fitting scheme. This is further complicated by the fact that the line shapes of transitions involving the valence band are not known *a priori*. For several peaks, particularly the As $M_{45}VV$ transition, the background exhibits different shapes for different surface phases, necessitating background subtraction before line-shape comparisons can be made. Here we have used a simplified approach by approximating the background under the peak with a straight line. Obviously, this will not yield the true line shape. However, the method employed here will suffice in the present comparative analysis.

III. OVERVIEW OF THE III-V LOW-ENERGY AUGER SPECTRA

The Auger transitions of the III-V compound system can be divided into a low- and a high-energy set which for GaAs appear below 160 and above 900 eV, respectively. From the escape-depth curve of GaAs,⁴ which has its minimum at about 50 eV, we find that the low-energy peaks appear in a very favorable range for use in surface studies. This high surface sensitivity is our motivation to look to detail at the low-energy spectrum in this paper. In Fig. 1 we present a calculation of all possible Auger transitions below 170 eV kinetic energy for the III-V elements Ga, Al, In, As, P, and Sb. It is worth noting that our aim has not been to provide accurate energy values of the Auger transitions but to investigate the relative positions of all possible peaks. This information is important when selecting a material suitable for experimental investigations of *CCV* and *CVV* peaks due to their large width and possible overlap. To calculate the kinetic energy of a transition I-II-III, the formula

$$E(\text{I-II-III}) = E(\text{I}) - E(\text{II}) - E(\text{III}) - U_{\text{eff}} \quad (1)$$

has been used with the binding energies E taken from x-ray experiments.⁵ Owing to the two holes left behind the escaping Auger electron, the kinetic energy is diminished by a correlation energy U_{eff} as compared to the one-electron value. This effect is comparatively large in GaAs and, furthermore, varies with the type of transition (*CCC*, *CCV*, or *CVV*). We have taken this effect into account in an empirical way by decreasing all *CCC* one-electron energies by 20 eV, as measured for the As $M_{23}M_{45}M_{45}$ peaks in GaAs, and the *CCV* and *CVV* transitions by 5 eV obtained from As $M_{45}VV$ and $M_1M_{45}V$ peaks also from GaAs. This difference between *CCC* transitions and those involving valence electrons can be understood by the difference in localization of the holes. When a hole appears in the valence band it will be less well localized and thus exert a smaller attractive force on the Auger electron. For all materials a valence-band width of 15 eV was used. The results are displayed in Fig. 1.

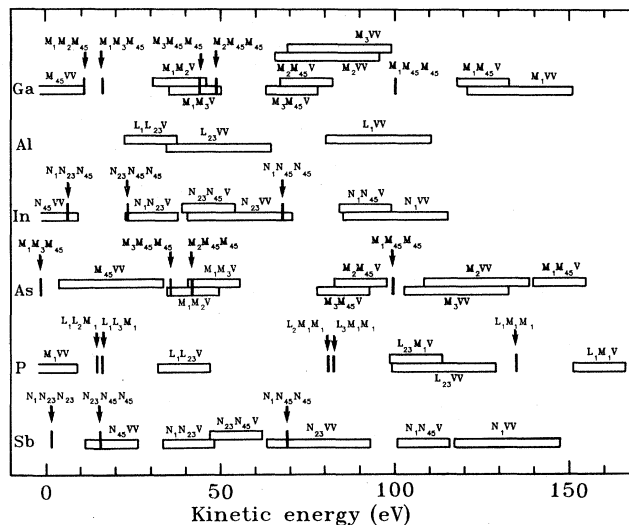


FIG. 1. Estimated energies of the spectral distribution of Auger transitions from the III-V elements Ga, Al, In, As, P, and Sb. For details about the calculations, see the text.

To study the line shape of the *CVV*-type transitions of III-V compounds we can use Fig. 1 to select a favorable material combination. The P $L_{23}VV$ peak, for example, could be easily studied in AlP or InP, where the group-III elements would not interfere with the studied peak. InP, in particular, is a favorable material since the intensities of the low-energy In transitions are very weak. Furthermore, the Al $L_{23}VV$ peak may be studied in AlAs since only the As $M_1M_{23}V$ peaks, showing extremely low intensity, will interfere with the low-energy part of the Al peak. The part of the intense As $M_{45}VV$ transition that falls outside the secondary electron peak can be studied in GaAs as well as in AlAs. The $M_{45}VV$ and $L_{23}VV$ peaks from Al and As are often used in surface studies. They are also favorable for testing line-shape models since they represent elements from both groups III and V. In Sec. V we will present our calculated and measured line shapes for these peaks. The strongest Ga transitions in the low-energy range are the $M_{23}M_{45}M_{45}$ peaks. Owing to the frequent use of these peaks in surface studies, we will continue here to describe their line shape.

IV. INTERPRETATION OF THE Ga $M_{23}M_{45}M_{45}$ PEAKS

Looking in detail at the Ga $M_{23}M_{45}M_{45}$ peaks of GaAs, one observes the expected two main peaks as well as another additional feature on the high-energy flank. In Fig. 2 this spectral range is displayed as obtained from GaAs and pure Ga. The background approximation is shown in the inset of Fig. 2. The applicability of this approach could be questioned, particularly for GaAs in view of the fact that also the $M_1M_{23}V$ peaks from both Ga and As should coincide with the Ga peaks (cf. Fig. 1). However, by observing the overall shape of the background, we estimate the error to be small. This conclusion is corroborated by the direct observation of the low intensity of the Ga M_1M_2V transition appearing below 45 eV in the pure-Ga spectrum (cf. Figs. 1 and 2).

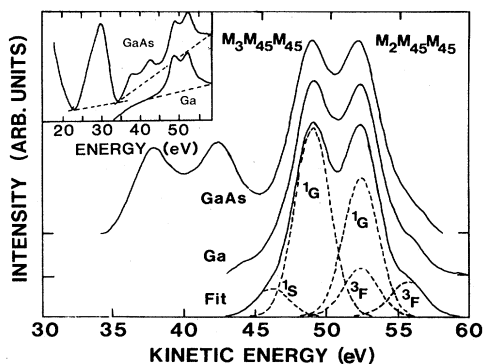


FIG. 2. Ga $M_{23}M_{45}M_{45}$ Auger peaks obtained from (a) GaAs and (b) metallic Ga. Curve (c) is a fit of five Gaussians to the metallic Ga spectrum. In the inset are shown the measured spectra before background subtraction. The linear background approximation is indicated with the dashed lines.

The multiplet splitting of the possible final states of the $M_{23}M_{45}M_{45}$ peaks are 1S , 3P , 1D , 3F , and 1G . Comparing these Ga peaks with the corresponding spectrum from Zn (Ref. 6) or $L_{23}M_{45}M_{45}$ from Ga (Ref. 7), we can identify the main peak as the 1G final state and the high-energy feature as the 3F multiplet final state. In the pure-Ga spectrum the 1S peak from the $M_2M_{45}M_{45}$ transition is also observed, which, however, is obscured in GaAs by the As MMM transitions as seen in Fig. 2. From considerations of the statistical occupation of the M_2 and M_3 levels, which is 1:2, one expects the $M_3M_{45}M_{45}$ peak to be twice as high as $M_2M_{45}M_{45}$. In the present case, as well as in Zn, the observed spectrum consists of two main peaks of approximately equal size. This is partly due to the fact that the $M_3M_{45}M_{45}$ 3F line coincides with the $M_2M_{45}M_{45}$ 1G peak. To estimate the size of the different contributions, we fitted five Gaussians to the metallic Ga spectrum. As restrictions on the fit we gave all peaks the same width (2.9 eV) and required the 1G -to- 3F peak-height ratio to be identical for the two transitions. We then obtained the signal ratios $^1G: ^3F=4$ and $^1G(M_3): ^1G(M_2)=1.4$. The latter value deviates considerably from the statistical value 2, a condition also found for Zn. Although the background subtraction may affect this value, as will the fact that the other multiplet states have been neglected, we find it clear that the ratio is indeed smaller than 2. The explanation for this is not known.⁶

Finally, we note that the similarity between the line shapes of the MMM peaks obtained on GaAs and pure Ga shows that the chemical environment does not significantly affect their shapes (although an energy shift between pure Ga and GaAs does appear). Information about the Ga content of the GaAs surface extracted from intensity measurements of these peaks should therefore be reliable.

V. INTERPRETATION OF CVV SPECTRA

A. Calculations of CVV transitions

As no core hole is present in the final state of a CVV process (in contrast to the case of CCV), the line shape

may be described in the one particle approximation using conventional band-structure concepts. Theories within this framework are expected to reproduce experimental data well if the effective hole-hole Coulomb repulsion U_{eff} is small compared to the full valence-band width Γ . On the other hand, when $U_{\text{eff}} > \Gamma$ the line shape will be atomiclike.⁸ We will assume the former situation to be true in our case. Our assumption is based on the estimate of the correction term to Eq. (1) (~ 5 eV) as compared to the bandwidth above the heteropolar gap (~ 7 eV). The approximation is probably good for the shape of the top part of the valence band. As will be further discussed below, the low-lying, more localized As s states are expected to be shifted to higher binding energies due to a larger U_{eff} .

An independent-particle formulation for valence-band Auger emission has been presented by, e.g., Feibelman *et al.*⁹ In this theory the local density of states (LDOS) enters as partial-density-of-states matrices. The Auger current is obtained as a convolution of these matrices weighted by transition probabilities. In a later paper Feibelman and McGuire¹⁰ showed that the Auger current, to a good approximation, often can be expressed in terms of the diagonal part of the density-of-states matrices, i.e., the conventional local partial density of states. This approach is employed here. The line shape can then be written as a linear combination of density-of-states self-fold contributions. It has also been found that for different materials these contributions attain approximately the same relative strength ratio.¹¹ Incidentally, the ratios are similar to what is found for the ratios between the decay-channel numbers obtained by considering the selection rules for the Auger transition,⁹ i.e., conservation of parity and angular momentum.

We have obtained the band structure by empirical tight-binding calculations based on the formalism due to Chadi and Cohen.¹² In this model, wave functions are constructed from linear combinations of atomic s and p waves of Ga and As. The Hamiltonian, corrected for printing errors in the original paper, is listed in the Appendix. The GaAs parameters were fitted to photoemission data from Chiang *et al.*¹³ In the case of AlAs, calculated values by Froyen and Cohen¹⁴ were used. In the fitting scheme the conduction-band energies were not accurately fitted in order to improve the accuracy of the fit of the valence-band energies. The fitting was successful to approximately 0.1 eV. The angular-momentum-resolved density-of-states function was obtained by generating random k vectors. For later reference we show the total density of states for GaAs in Fig. 3. The result is close to that of Jarlborg and Freeman, who made a full, self-consistent linear muffin-tin orbital (LMTO) calculation.¹⁵ Three peaks are observed. Peak I derives mainly from the atomic As s state. The other part of the valence band originates from a complicated mixture in the region of the atomic Ga s and As p states. Peak II is atomically associated with the Ga s but in the solid state also contains As p character through tails from the Ga p states. Similarly, the large peak III derives from As p but also contains Ga p character through hybridization. We note that Jarlborg and Freeman¹⁵ obtain a somewhat higher amplitude for

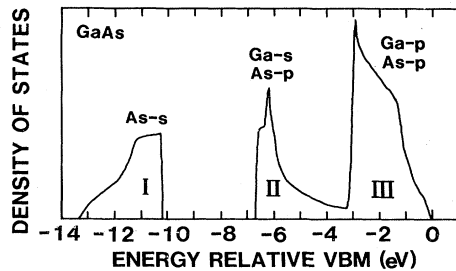


FIG. 3. Total valence-band density of states of GaAs as obtained from an empirical tight-binding calculation. Energies are given relative to the valence-band maximum (VBM). The origin of the features denoted I, II, and III is discussed in the text.

peak II as compared to peak III than we do.

The various self-folds for the group-III and -V elements are displayed in Fig. 4 as obtained from the AlAs band structure. Auger electrons appearing due to holes located above the heteropolar band gap are emitted with an energy above the lines marked *G* (denotes gap) in the figure. As will be seen in comparison with experiments, information about the hole origin is important since below the heteropolar gap, holes can be expected to be more localized, making the band picture an unsatisfactory way of describing the Auger transition.

For the group-V elements, Fig. 4(a), the uppermost, large *pp* peak is essentially a self-fold of peak III in Fig. 3, while the smaller *pp* peak is a fold of peaks II and III. The strong *sp* peak derives from a fold of peak III with the low-lying *s*-derived peak I. Note that in the case of the group-III element Al, Fig. 4(b), the strongest *sp* peak is situated at higher energy than in the group-V case and, in fact, coincides with the second-highest *pp* peak. Furthermore, in contrast to the case of the group-V element, the largest *sp* peak originates from states above the heteropolar gap.

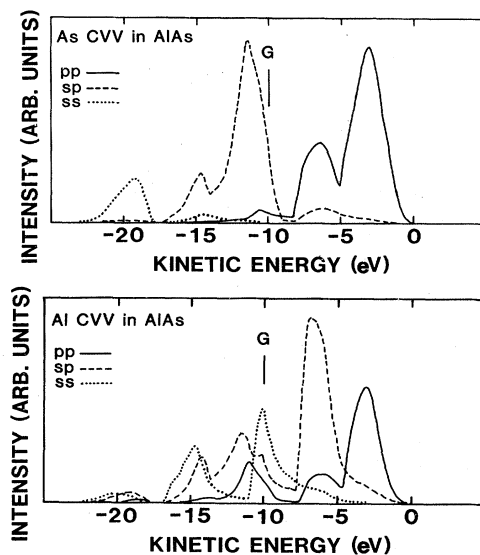


FIG. 4. As and Al *ss*, *sp*, and *pp* self-folds of the local density of states obtained from the empirical tight-binding calculation of AlAs. Above *G* at 10 eV the involved hole states are situated above the heteropolar gap.

The calculated GaAs As $M_{45}VV$ Auger spectrum is shown in Fig. 5, curve *c*. The transition probabilities enhance the *pp* contributions over those from *sp* and *ss* folds. In the experiment a further enhancement of the high-energy part is observed when using a cylindrical mirror analyzer, since the signal from this instrument is proportional to $EN(E)$. Here, E is the kinetic energy and $N(E)$ is the emitted Auger-electron distribution. All calculated Auger spectra are presented with the relative transition probabilities $ss:sp:pp=0.03:0.3:1$ for the self-fold contributions,¹¹ as well as with $EN(E)$ weighting. The transition probabilities are given for *KLL* and *LMM* transitions only, in Ref. 11, but in both cases the *sp*-to-*pp* ratio is about 0.3. It is assumed that this is also true in our case. The *ss* contribution is very small and its exact relative contribution is not very important here.

B. Experimental results and comparison with theory

The density of states of the III-V compounds appear very similar, with only minor differences in the band widths. Hence the line shape of Auger transitions from each group (III or V) will also resemble each other. We therefore first compare the line shape of the group-V element As in different chemical surroundings, and then present the results for the group-III element Al.

1. As $M_{45}VV$ in As, GaAs, and AlAs

The linear background approximation for the *CVV* peaks is illustrated in the inset of Fig. 2. In the case of the As *MVV* peak the method can obviously only extract the part of the transition appearing above the large secondary-electron peak. The experimental and theoretical As *MVV* peaks from GaAs, As, and AlAs are shown in Figs. 5 and 6. The calculated spectrum is considerably sharper than the experimental one. Allowing for lifetime broadening of the core state, as well as the two valence hole states, is not sufficient to account for this discrepancy. We propose that the hole-hole correlation effect manifested through U_{eff} in Eq. (1) causes an extra broadening

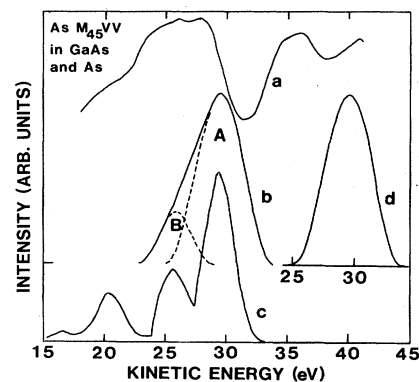


FIG. 5. Experimental and theoretical line shapes of the As $M_{45}VV$ transition from GaAs. The uppermost curve, (a), shows the derivative spectrum. Curve (b) is the corresponding, background-reduced and decomposed experimental line shape. The spectrum obtained from amorphous As is shown as curve (c). The lowest curve, (d), is the calculated, weighted line shape.

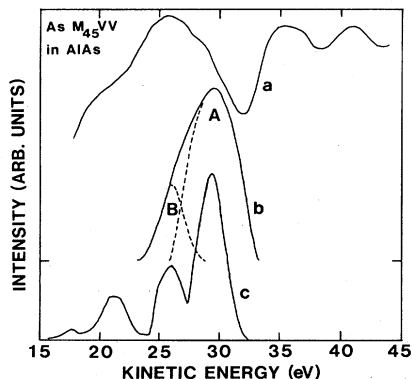


FIG. 6. Experimental and theoretical line shapes of the As $M_{45}VV$ transition from AlAs. Curve (a) is the differentiated spectrum. The integrated, background reduced and decomposed line shape is shown as curve (b). The calculated line shape is displayed as curve (c).

mechanism which could be described by the imaginary part of the appropriate self-energy. Knowing from the theory that the main peak should consist of two approximately symmetric peaks, we have artificially broken down the experimental peak by first creating a mirror image of the high-energy flank. This produces a peak that we hereafter denote *A*. Subtracting the *A* peak from the experimental peak yields a smaller peak (that we call *B*) which turns out to be symmetric. The result of this breakdown is shown in Figs. 5 and 6, curves *b*. We see that the separation between the *A* and *B* peaks agrees almost perfectly with the separation between the calculated peaks for both GaAs and AlAs, namely 3.7 and 3.4 eV, respectively. The smaller separation in AlAs is basically a consequence of the narrower width of the topmost bands in AlAs as compared with GaAs. Although the difference in peak separation between the two materials is small, a characteristic line-shape difference is observed in the differentiated spectrum. An application of this fact is exemplified in Al adsorption experiments on GaAs(001), where the line shape is seen to change from typical GaAs to AlAs character,¹⁶ supporting the previous findings by Landgren *et al.*¹⁷ of AlAs formation in the submonolayer range. In the derivative spectrum some *sp* features are also discernible, although the low signal strength and our inability to subtract a background in this interval makes detailed comparison impossible. As mentioned above, these structures may, however, be distorted due to possible localization of the hole below the heteropolar gap. By studying the P $L_{23}VV$ line in InP, the entire spectrum from a group-V element can, however, be studied. Such investigations are in progress and will be presented elsewhere.¹⁸ In contrast to the case of GaAs, the As MVV peak from amorphous As appears almost completely symmetric, as seen in Fig. 5, curve *d*. Moreover, its width and shape are identical to peak *A* of the decomposed GaAs spectrum. For amorphous As the density of states (DOS) as observed in ultraviolet photoemission spectroscopy¹⁹ (UPS) or x-ray photoemission spectroscopy²⁰ (XPS) is, however, not symmetric. To a first approximation this DOS resembles the As *p* part in GaAs. One might therefore expect an MVV transition from pure As to show a

line shape similar to that obtained from GaAs. As this is not observed experimentally, we are inclined to believe that the *p* part of the pure-As local density of state (LDOS) is, in fact, symmetric (mirroring peak I in Fig. 3), and that the residual part of the As DOS exhibits mainly *s* character.

2. GaAs composition dependence of the As $M_{45}VV$ peak

Starting from an As-rich GaAs(001) surface phase, a temperature increase leads to a net desorption of As, while the surface structure remains ordered up to the congruent evaporation point^{21,22} ($\sim 660^\circ\text{C}$). In such experiments the As-to-Ga Auger signal ratio is seen to decrease smoothly and continuously, while rather abrupt changes in surface symmetry are observed. We find that the order in which the surface reconstructions appear basically follows the order determined by Cho.²³ This and the decreasing As-to-Ga signal ratio is consistent with the composition order of the reconstructions as given by Drahten *et al.*,²⁴ but at variance with that given for the Ga-rich reconstructions by Bachrach *et al.*²⁵

AES has been used extensively for quantitative measurements of the [As]/[Ga] composition of GaAs surfaces. Hence it is very important to investigate the reliability of such analyses. All M_{45} core holes created at an As site will decay via an $M_{45}VV$ transition. The total number of emitted MVV Auger electrons is therefore proportional to the integrated area under the entire spectrum, consisting of all *pp*, *sp*, and *ss* contributions. However, as seen in Fig. 5, in experiments we can only observe the *pp* part. A rehybridization of the surface-atom bonds induced by changing composition will change the distribution of electrons between *s* and *p* states. Thus the *pp*-fold will not be strictly proportional to the total number of MVV electrons during a composition change. At present we cannot determine the magnitude of this effect since it would require detailed surface band-structure calculations. As we have already seen above, a quite considerable difference in the As LDOS is observed when comparing GaAs and amorphous As. Therefore we do not expect GaAs surfaces with adsorbed As to give As MVV signals that are proportional to the As concentration and comparable with signals from clean GaAs surfaces. For surfaces where As is bonded to Ga, the situation may be somewhat more favorable in the sense that the *s*-to-*p* redistribution may not be that large. The low *sp:pp* transition probability ratio further helps to diminish any effect from an unproportional change in the *sp* area. (It has been shown that the transition probabilities do not change between solid and gaseous phases.¹¹ Hence we can assume that they will also remain unchanged between different solid surface phases.) We can then expect the observable *pp*-fold to be approximately proportional to the total area of the $M_{45}VV$ peak, being a measure of the As concentration.

It is of further interest to see to what degree the derivative peak-to-peak height is proportional to the *pp* peak area. The change in peak shape from As to GaAs character during the phase change can be seen as an increase in the *B/A* peak area ratio (cf. Fig. 5). It is apparent that

this increase will diminish the "up peak" in the first-derivative spectrum. We then expect the peak-to-peak signal to give an underestimate of the total peak area. We have followed the development of the error by measuring the difference between the integrated peak area and the peak-to-peak height, normalizing each signal type at the lowest temperature at which the Auger peak is most symmetric. Although there is scatter in the data, the difference development supports the expected underestimate of the peak-to-peak-height method. The maximum difference is about 5%. Thus the accuracy of an analysis of differentiated spectra seems to be comparable to that of directly obtained spectra. The main uncertainty in the data is related to the degree of rehybridization.

In our heating experiments of As-rich GaAs(001) $c(4 \times 4)$ surfaces, the line shape of the MVV peak was observed to change from mainly pure-As character (symmetric) to strong GaAs character (asymmetric). Furthermore, we observe highly varying initial As-to-Ga Auger intensities for this structure at room temperature. These facts are in qualitative agreement with the view of the $c(4 \times 4)$ structure consisting of an adsorbed As layer of varying coverage on top of the GaAs surface.²⁶ We have rationalized the observation of an increasing B peak by subtracting from each GaAs spectrum an As spectrum scaled to the height of the A part to simulate the main pp peak. The area of the residual peak (B) was then compared with the area of the total peak area ($A+B$). Note that, for all investigated spectra, the resulting B peak remained symmetric and separated the same distance (3.7 eV) from the A peak, supporting the applicability of the adopted decomposition method. In Fig. 7 we have plotted the $(As M_{45}VV)/(Ga M_2M_{45}M_{45})$ first-derivative peak-to-peak signal ratio as a function of the MVV area ratio $(A+B)/B$. Both sets of data were normalized at the As-to-Ga Auger signal-strength ratio, 2.12, obtained for the $c(2 \times 8)$ reconstruction. This is a mean value around which we have found high-quality $c(2 \times 8)$ surfaces to appear in a narrow range. The quality here is judged from the appearance of a RHEED pattern showing a highly or-

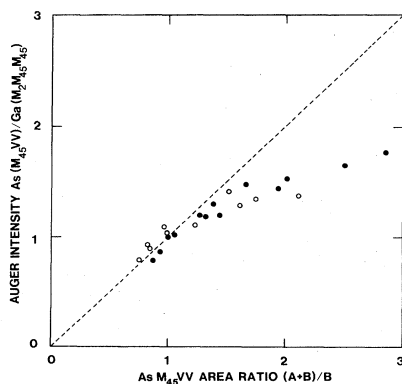


FIG. 7. Auger signal ratio for the $(As M_{45}VV)/(Ga M_2M_{45}M_{45})$ peak-to-peak derivative signals plotted as a function of the $As M_{45}VV$ decomposed peak area ratio $(A+B)/B$. The open and solid circles represent two different $c(4 \times 4)$ reconstructed samples with different initial As content. For details about the normalization, see the text.

dered surface (short streaks and high signal-to-background intensity). The ratio 2.12 is close to the value 2.10 obtained on the cleavage plane (110) of GaAs,²⁴ which is known to be stoichiometric. Also, other investigators have found the $c(2 \times 8)$ surface to be close to stoichiometric.^{24,27} Figure 7 shows a strong relationship between the Ga concentration and the B peak. The line shape changes continuously and can be described directly in terms of changes in the band structure induced by the chemical surrounding of the As atom. The change in the A -to- B peak intensity is due to a change in intensity between the As part of the two topmost GaAs valence bands (peaks II and III, Fig. 3). The same trend has been observed also in angle-integrated photoemission spectra,²⁵ as well in CCV Auger line shapes.²⁸ In the photoemission spectra an increase in peak II (Fig. 3) can, however, be due to changes in both the Ga and As contributions.

3. The $Al L_{23}VV$ transition

The Auger transitions of group-III elements show a more complex mixture of pp - and sp -folds, as seen in Fig. 4(b). In the calculated Auger spectrum, Fig. 8, the second-highest peak derives from the sp -fold rather than from a pp -fold as in the group-V-element case. For Al we must also consider the separation between the L_2 and L_3 levels are (1 eV), adding the two separate L_2VV and L_3VV transitions to give the resulting line shape. With the same weighting as above, our calculated spectrum yields a fair reproduction of the topmost structure of the line shape. However, the pp structure appearing around the middle of the transition is not identified in the experiment (cf. Fig. 8). This latter structure is a fold of the topmost and lowest valence bands in AlAs. The hole created in the lowest valence band, corresponding to peak I in Fig. 3, will be quite localized. Thus the transition tends towards one of CCV character with a quasilocized hole in the final state. This should give rise to an increased binding energy of the Auger electron as compared to the calculated value. The observed peak around 47 eV is a candidate for the third uppermost calculated structure. Unfortunately, the underlying $L_1L_{23}V$ transition may obscure a detailed analysis. The corresponding effect in $L_{23}VV$ of P in InP seems clearer.¹⁸

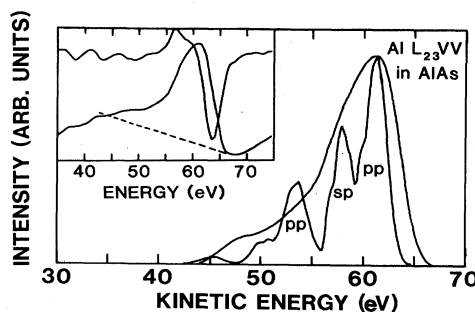


FIG. 8. Experimental and theoretical line shapes of the $Al L_{23}VV$ transition from AlAs. The inset shows the derivative and direct spectra. The dashed line indicates the background simulation.

VI. DISCUSSION

In the preceding sections we have seen that the Auger *CVV* peak line shapes from the III-V compounds can be described with a band-structure model for the valence electrons above the heteropolar gap. With the present investigation, together with the previous work on the *CCV* transitions,^{29,30} we can state that we now possess a fairly good understanding of all low-energy Auger spectra from GaAs. We have seen that the line shape of the As *MVV* peak contains information about the chemical surrounding of the As atom. The merits of an AES line-shape analysis can be exemplified by our observation of *c*(2×8) reconstructed GaAs surfaces with As-to-Ga signal ratios exceeding 2.12 (cf. above discussion) and with As *MVV* line shapes with pronounced As character. We interpret this as strong evidence for the presence of a disordered, dilute adlayer of As on top of a nearly stoichiometric GaAs surface. As the same conditions have also been observed on the Ga-rich *c*(4×6) reconstructed surface, we have been led to conclude that "extra" disordered As is the main problem in achieving a reproducible surface composition in MBE production of surfaces. It can be noted that during prolonged annealing we have also obtained *c*(2×8) reconstructed surfaces with signal ratios below 2. Hence, variations in measured surface composition may not solely originate from excess As but also from material deficiencies in the surface. More detailed LDOS calculations considering varying surface compositions together with line-shape studies of the As *MVV* peak may prove fruitful in the determination of the ideal As-to-Ga signal ratio for a specific reconstruction. Here it should be mentioned that information about the site-specific GaAs LDOS may also be obtainable using *CCV* transitions. The distortion of the LDOS due to the core hole in the final state should then be considered. Also, the weak signal strength of these peaks requires considerable longer data-sampling times, as mentioned by Davis *et al.*²⁸ (~1 h). For detailed studies of the GaAs(001) surface phases, as exemplified in Fig. 7, time considerations then make the *CVV* peak a more useful surface probe.

VII. SUMMARY

We have shown that a weighted self-fold of the site-specific angular-momentum-resolved density of states for III-V compounds well describes the topmost part of the *CVV*-type Auger spectra. In the case of the As *M₄₅VV* transition, the line shape carries information about the chemical surrounding of the As atom that can be used for studies of different surface phases of GaAs. Using this technique we have identified adsorbed As on top of a *c*(2×8) reconstructed GaAs(001) surface, as well as AlAs formation during Al adsorption on GaAs. The Ga *MMM* peaks can, to a first approximation, be described each with two Gaussians representing the strongest multiplet final states. The intensity ratio between the *M₂* and *M₃* lines deviates from the expected statistical value of 2. The line shapes of the Ga *MMM* and As *MVV* peaks are such that intensity ratios from differentiated spectra should give reliable information about the surface composition of a GaAs surface.

ACKNOWLEDGMENTS

This work was financed by the Swedish Board for Technical Development and the Swedish Natural Research Council.

APPENDIX

Here we list the Hamiltonian matrix used for the calculation of the linear combination of atomic orbitals band structure. In the original matrix, as presented by Chadi and Cohen,¹² some of the elements suffer from printing errors. These have been corrected and are underlined here. We note that if the band diagram is calculated between the Γ point and the *X* point ($2\pi/a, 0, 0$), both the erroneous and correct matrices give the same results. For other equivalent *X* points [e.g., ($0, 2\pi/a, 0$)], different results are obtained. We present the matrix (*c* denotes cation; *a* denotes anion):

| | S^c | S^a | P_x^c | P_y^c | P_z^c | P_x^a | P_y^a | P_z^a |
|---------|---------------|--------------|---------------------------|----------------|---------------------------|-------------------------|-------------------------|-------------------------|
| S^c | E_s^c | $E_{ss}g_0$ | 0 | 0 | 0 | $E_{sp}g_1$ | $E_{sp}g_2$ | $E_{sp}g_3$ |
| S^a | $E_{ss}g_0^*$ | E_s^a | $-E_{sp}g_1^*$ | $-E_{sp}g_2^*$ | $-E_{sp}g_3^*$ | 0 | 0 | 0 |
| P_x^c | 0 | $-E_{sp}g_1$ | E_p^c | 0 | 0 | $E_{xx}g_0$ | $E_{xy}g_3$ | $\underline{E_{xy}g_2}$ |
| P_y^c | 0 | $-E_{sp}g_2$ | 0 | E_p^c | 0 | $E_{xy}g_3$ | $E_{xx}g_0$ | $\underline{E_{xy}g_1}$ |
| P_z^c | 0 | $-E_{sp}g_3$ | 0 | 0 | E_p^c | $\underline{E_{xy}g_2}$ | $\underline{E_{xy}g_1}$ | $E_{xx}g_0$ |
| P_x^a | $E_{sp}g_1^*$ | 0 | $E_{xx}g_0^*$ | $E_{xy}g_3^*$ | $\underline{E_{xy}g_2^*}$ | E_p^a | 0 | 0 |
| P_y^a | $E_{sp}g_2^*$ | 0 | $E_{xy}g_3^*$ | $E_{xx}g_0^*$ | $\underline{E_{xy}g_1^*}$ | 0 | E_p^a | 0 |
| P_z^a | $E_{sp}g_3^*$ | 0 | $\underline{E_{xy}g_2^*}$ | $E_{xy}g_1^*$ | $\underline{E_{xx}g_0^*}$ | 0 | 0 | E_p^a |

*Present address: Gould Research Center, 40 Gould Center, Rolling Meadows, IL 60008.

¹S. P. Svensson, J. Kanski, T. G. Andersson, and P.-O. Nilsson, *J. Vac. Sci. Technol. B* 2, 235 (1984).

²W. I. Wang, *J. Vac. Sci. Technol. B* 1, 574 (1983).

³T. P. Hult, S. P. Svensson, and T. G. Andersson, *Comput. Phys. Commun.* 25, 417 (1982).

⁴I. Lindau and W. E. Spicer, *J. Electron. Spectrosc. Relat.*

- Phenom. **3**, 409 (1974).
- ⁵F. P. Larkins, *At. Data Nucl. Data Tables* **20**, 311 (1977).
- ⁶M. Ohno and G. Wendin, *J. Phys. B* **12**, 1305 (1979), and references therein.
- ⁷E. Antonides, E. C. Janse, and G. A. Sawatsky, *Phys. Rev. B* **15**, 1669 (1977).
- ⁸M. Cini, *Phys. Rev. B* **17**, 2788 (1978); G. A. Sawatsky, *Phys. Rev. Lett.* **39**, 504 (1977).
- ⁹P. J. Feibelman, E. J. McGuire, and K. C. Pandey *Phys. Rev. B* **15**, 2202 (1977).
- ¹⁰P. J. Feibelman and E. J. McGuire, *Phys. Rev. B* **17**, 690 (1978).
- ¹¹D. E. Ramaker, in *Chemistry and Physics of Solids IV*, edited by R. Vanselow and R. Howe (Springer, Berlin, 1982).
- ¹²D. J. Chadi and M. L. Cohen, *Phys. Status. Solidi.* **68** 405 (1975).
- ¹³T.-C. Chiang, J. A. Knapp, M. Aono, and D. E. Eastman, *Phys. Rev. B* **21**, 3513 (1980).
- ¹⁴S. Froyen and M. L. Cohen, *Phys. Rev. B* **28**, 3258 (1983).
- ¹⁵T. Jarlborg and A. J. Freeman, *Phys. Lett.* **74**, 349 (1979).
- ¹⁶S. P. Svensson (unpublished).
- ¹⁷G. Landgren, S. P. Svensson, and T. G. Andersson, *Surf. Sci.* **122**, 55 (1982).
- ¹⁸P. O. Nilsson and S. P. Svensson (unpublished).
- ¹⁹C. Y. Su, I. Lindau, P. R. Skeath, I. Hino, and W. E. Spicer, *Surf. Sci.* **118**, 257 (1982).
- ²⁰L. Ley, R. A. Pollak, S. P. Kowalczyk, F. R. McFreely, and D. A. Shirley, *Phys. Rev. B* **8**, 641 (1973).
- ²¹C. T. Foxon, J. A. Harvey, and B. A. Joyce, *J. Phys. Chem. Solids* **34**, 1693 (1973).
- ²²B. Goldstein, D. J. Szostak, and V. S. Ban, *Surf. Sci.* **57**, 733 (1976).
- ²³A. Y. Cho, *J. Appl. Phys.* **47**, 2841 (1976).
- ²⁴P. Drahten, W. Ranke, and K. Jacobi, *Surf. Sci.* **77**, L162 (1978).
- ²⁵R. Z. Bachrach, R. S. Bauer, P. Chiaradia, and G. V. Hansson, *J. Vac. Sci. Technol.* **18**, 797 (1981).
- ²⁶P. K. Larsen, J. H. Neave, J. F. van der Veen, P. J. Dobson, and B. A. Joyce, *Phys. Rev. B* **27**, 4966 (1983).
- ²⁷R. Ludeke, T.-C. Chiang, and D. E. Eastman, *Physica (Utrecht)* **117&118B**, 819 (1983).
- ²⁸G. D. Davis, D. E. Savage, and M. G. Lagally, *J. Electron Spectrosc. and Relat. Phenom.* **23**, 25 (1981).
- ²⁹P. J. Feibelman, E. J. McGuire, and K. C. Pandey, *Phys. Rev. B* **16**, 5499 (1977).
- ³⁰G. D. Davis and M. G. Lagally, *J. Vac. Sci. Technol.* **15**, 1311 (1978).